# Analytical performance assessment of 1-D ESPRIT in DFT beamspace in terms of physical parameters

*Damir Rakhimov and Martin Haardt*
Communications Research Laboratory, Ilmenau University of Technology,
P. O. Box 100565, D-98684 Ilmenau, Germany
Emails: {damir.rakhimov, martin.haardt}@tu-ilmenau.de

***Abstract*—In this paper, we present an asymptotic performance analysis of a subspace-based parameter estimation scheme in DFT beamspace that is based on a first-order expansion of the estimation error that is due to additive noise. We provide a general expression of the mean squared error (MSE) for 1-D ESPRIT in DFT beamspace as a function of the perturbation in terms of physical parameters, such as the array steering matrix, the beamforming matrix, the signal correlation, the number of snapshots, and the size of the array. Additionally, a closed-form expression is provided for the case of a single source. This paper includes the main parts of the derivation. For the simulation results, we compare the analytical performance with the empirical one that is based on Monte-Carlo trials. We also compare the performance of the DFT beamspace version with the element space counterpart of the ESPRIT algorithm and reveal the benefits of the former. In conclusion, we discuss possible extensions for follow-up investigations.**

***Index Terms*—1-D ESPRIT in DFT Beamspace, harmonic retrieval, performance assessment, first-order perturbation analysis.**

## I. Introduction

In recent years, there has been renewed interest in the development of high-resolution parameter estimation techniques for applications related to the next-generation wireless communication systems operating in the millimeter frequency range. As a result, the importance of theoretical performance analysis for algorithms increases, especially to justify the choice among various potential candidates. The first-order perturbation method represents a powerful tool to compare the efficiency of various direction of arrival (DOA) estimation algorithms and methods. It was applied to the analysis of various subspace-based algorithms, such as MUSIC, ESPRIT, and Min-Norm in [1]–[3]. It was also successfully extended to the analysis of multidimensional algorithms in [4]–[7].

In this paper, we derive the performance analysis for the 1-D ESPRIT in DFT Beamspace described in [8] based on the explicit first-order expansion of the estimation error in the signal subspace that is due to additive noise. It differs from the ones presented in [9], [10], and [11]. In [9], the authors exploit a different approach that is based on the distribution of the eigenvectors of a sample covariance matrix [12]. The performance assessment based in [12] is asymptotic in the number of snapshots $N$ and relies on strong Gaussianity assumptions on the source symbols and the noise. In [10], authors consider the beamspace transformation applied to separate subarrays. This differs from our system model, where we apply beamforming to the complete aperture. In [11], authors describe the multidimensional extension of [8] and present the performance analysis for it. However, the expressions presented in this paper are more accurate and have a simpler expression than the one presented in [11]. Furthermore, the performance analysis in [11] is derived in terms of signal subspaces which makes the application of the resulting expressions more difficult. Moreover, the presented in this paper expressions are derived in terms of physical parameters which simplifies the calculation in comparison to the results presented in [4]–[6], [11]. They can also be applied to the analysis of multidimensional extensions of Beamspace ESPRIT in [13] or [11].

The contributions of the paper are the following:

- We derive expressions in terms of physical parameters for the asymptotic performance analysis of 1-D ESPRIT in DFT beamspace using an explicit first-order expansion of the estimation error.
- We derive a closed-form expression of the mean squared error (MSE) for the case of a single source.
- We show the impact of the number of snapshots as well as the size of the array aperture on the performance of the algorithm.

For this work, we follow the notation established in [11], [13], [14].

## II. System model

We consider a uniform linear array of $M$ isotropic antennas and inter-element spacing $\Delta = \frac{\lambda}{2}$. We assume that $d$ plane-wave signals impinge on the array. The received signal consists of $N$ snapshots. Its element space formulation is given by

$$\tilde{\boldsymbol{Y}} = \boldsymbol{Y} + \boldsymbol{Z} = \boldsymbol{A}\boldsymbol{S} + \boldsymbol{Z} \in \mathbb{C}^{M \times N}, \tag{1}$$

where $\boldsymbol{Y} \in \mathbb{C}^{M \times N}$ is the noiseless version of the received signal, $\boldsymbol{A} \in \mathbb{C}^{M \times d}$ is the array steering matrix, the $i$-th column is a Vandermonde vector $\boldsymbol{a}_i = \begin{bmatrix} 1 & \mathrm{e}^{j\mu_i} & \dots & \mathrm{e}^{j(M-1)\mu_i} \end{bmatrix}^{\mathrm{T}}$, $\mu_i$ is the $i$-th spatial frequency, $\boldsymbol{S} \in \mathbb{C}^{d \times N}$ is the matrix of impinging signals with zero-mean, i.e., $\mathbb{E}\{\boldsymbol{S}\} = \boldsymbol{0}$, and covariance matrix $\boldsymbol{R}_{\mathrm{s}} = \mathbb{E}\left\{\frac{1}{N}\boldsymbol{S}\boldsymbol{S}^{\mathrm{H}}\right\} \in \mathbb{C}^{d \times d}$, and $\boldsymbol{Z}$ is the matrix with samples of noise.

Next, we perform the beamspace transformation of the received signals by applying a set of DFT beamformers to the outputs of the array

$$\tilde{\boldsymbol{Y}}_{\mathrm{DFT}} = \boldsymbol{W}^{\mathrm{H}}\tilde{\boldsymbol{Y}} = \boldsymbol{W}^{\mathrm{H}}(\boldsymbol{A}\boldsymbol{S} + \boldsymbol{Z}) = \boldsymbol{B}\boldsymbol{S} + \boldsymbol{W}^{\mathrm{H}}\boldsymbol{Z} \in \mathbb{C}^{M \times N}, \tag{2}$$

where $\boldsymbol{W} \in \mathbb{C}^{M \times M}$ is the matrix of DFT beamformers, the $\kappa$-th column is a column from the scaled DFT matrix of size $M \times M$ given by

$$\begin{aligned} \boldsymbol{w}_\kappa &= \mathrm{e}^{j\left(\frac{M-1}{2}\right)\kappa\frac{2\pi}{M}} \begin{bmatrix} 1 & \mathrm{e}^{j\kappa\frac{2\pi}{M}} & \mathrm{e}^{j2\kappa\frac{2\pi}{M}} & \dots & \mathrm{e}^{j(M-1)\kappa\frac{2\pi}{M}} \end{bmatrix}^{\mathrm{T}} \\ &= \mathrm{e}^{j\left(\frac{M-1}{2}\right)\gamma_\kappa} \begin{bmatrix} 1 & \mathrm{e}^{j\gamma_\kappa} & \mathrm{e}^{j2\gamma_\kappa} & \dots & \mathrm{e}^{j(M-1)\gamma_\kappa} \end{bmatrix}^{\mathrm{T}}, \end{aligned} \tag{3}$$

and $\gamma_\kappa = \kappa\frac{2\pi}{M}$, $0 \le \kappa \le (M-1)$, $\boldsymbol{B} = \boldsymbol{W}^{\mathrm{H}}\boldsymbol{A} \in \mathbb{C}^{M \times d}$ is the beamspace steering matrix, and $\boldsymbol{W}^{\mathrm{H}}\boldsymbol{Z}$ is the equivalent matrix with noise samples after the beamspace transformation. The matrix $\boldsymbol{W}$ is left $\boldsymbol{\Pi}$-real, i.e., $\boldsymbol{\Pi}\,\boldsymbol{W}^* = \boldsymbol{W}$, where $\boldsymbol{\Pi} \in \mathbb{R}^{M \times M}$ is the exchange matrix with ones on the anti-diagonal [8].

Note that to reduce the complexity of the beamspace version of the algorithm we use only a subset of columns from the beamforming matrix $\boldsymbol{W} \in \mathbb{C}^{M \times M}$ which comprises $B$ beamformers. Further in the paper we denote the subset of $B$ DFT beamformers as $\boldsymbol{W}_B \in \mathbb{C}^{M \times B}$. The particular beamformers of the subset can be determined via a sectorization procedure. An example of such a sectorization procedure can be found in [11]. An illustration of the beamspace transformation process is provided in Figure 1.

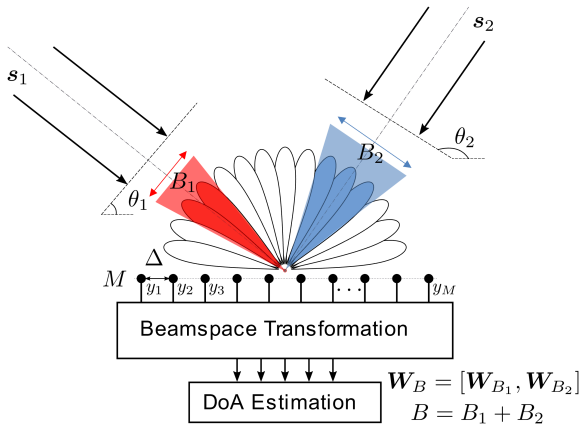


Fig. 1: Illustration on 1-D Beamspace transformation.

## III. Review of 1-D ESPRIT in DFT Beamspace

In this section, we provide a short summary of 1-D ESPRIT in DFT Beamspace [8]. First, we consider the noiseless case.

We start by calculating the singular value decomposition of the noiseless received signal $\boldsymbol{Y}_{\mathrm{DFT}} = \boldsymbol{U} \cdot \boldsymbol{\Sigma} \cdot \boldsymbol{V}^{\mathrm{H}}$ to estimate the signal subspace $\boldsymbol{U}_{\mathrm{s}}$. To this end, we compute $\boldsymbol{U}_{\mathrm{s}}$ as $d$ dominant left singular vectors of $\boldsymbol{Y}_{\mathrm{DFT}}$.

Following the derivation in [8], we can show that for a single source at the spatial frequency $\mu$, the output amplitudes $b_\kappa(\mu)$ and $b_{\kappa+1}(\mu)$ of two successive beams of the DFT beamspace manifold are related as

$$\left(\mathrm{e}^{-j\frac{1}{2}(\mu-\gamma_\kappa)} - \mathrm{e}^{j\frac{1}{2}(\mu-\gamma_\kappa)}\right) b_\kappa(\mu) + \left(\mathrm{e}^{-j\frac{1}{2}(\mu-\gamma_{\kappa+1})} - \mathrm{e}^{j\frac{1}{2}(\mu-\gamma_{\kappa+1})}\right) b_{\kappa+1}(\mu) = 0 \quad (4)$$

where $b_\kappa(\mu) = \boldsymbol{w}_\kappa^{\mathrm{H}} \boldsymbol{a}(\mu)$ and $b_{\kappa+1}(\mu) = \boldsymbol{w}_{\kappa+1}^{\mathrm{H}} \boldsymbol{a}(\mu)$. It leads to the shift-invariance equation

$$\mathrm{e}^{j\mu} \cdot \left\{\mathrm{e}^{-j\frac{1}{2}\gamma_\kappa} b_\kappa(\mu) + \mathrm{e}^{-j\frac{1}{2}\gamma_{\kappa+1}} b_{\kappa+1}(\mu)\right\} = \mathrm{e}^{j\frac{1}{2}\gamma_\kappa} b_\kappa(\mu) + \mathrm{e}^{j\frac{1}{2}\gamma_{\kappa+1}} b_{\kappa+1}(\mu) \quad (5)$$

Based on (5), we can write a shift-invariance equation for $d$ sources impinging on the array as

$$\boldsymbol{G}_{1,B} \boldsymbol{B} \boldsymbol{\Omega} = \boldsymbol{G}_{2,B} \boldsymbol{B} \in \mathbb{C}^{(B-1)\times d}, \quad (6)$$

where $\boldsymbol{\Omega} = \mathrm{diag}\left\{\mathrm{e}^{j\mu_i}\right\}_{i=1}^{d}$ is a diagonal matrix with spatial information, $\boldsymbol{G}_{1,B} \in \mathbb{C}^{(B-1)\times B}$ and $\boldsymbol{G}_{2,B} \in \mathbb{C}^{(B-1)\times B}$ are the selection matrices defined in (7). In the noiseless case, the matrix $\boldsymbol{B}$ and the received signals share the same subspace, i.e., $\boldsymbol{B} = \boldsymbol{U}_{\mathrm{s}} \boldsymbol{T}$, where $\boldsymbol{T}$ is a full rank matrix. Hence, we can write

$$\boldsymbol{G}_{1,B} \boldsymbol{U}_{\mathrm{s}} \underbrace{\boldsymbol{T} \boldsymbol{\Omega} \boldsymbol{T}^{-1}}_{\boldsymbol{\Upsilon}} = \boldsymbol{G}_{2,B} \boldsymbol{U}_{\mathrm{s}} \in \mathbb{C}^{(B-1)\times d}, \quad (8)$$

which we solve with respect to $\boldsymbol{\Upsilon}$ using the method of Least Squares (LS)

$$\boldsymbol{\Upsilon} = \left(\boldsymbol{G}_{1,B} \boldsymbol{U}_{\mathrm{s}}\right)^{+} \cdot \left(\boldsymbol{G}_{2,B} \boldsymbol{U}_{\mathrm{s}}\right) \in \mathbb{C}^{d\times d}. \quad (9)$$

Next, we find the diagonal entries of the matrix $\boldsymbol{\Omega}$ as eigenvalues of the matrix $\boldsymbol{\Upsilon}$

$$\boldsymbol{\Upsilon} = \boldsymbol{T}\, \boldsymbol{\Omega}\, \boldsymbol{T}^{-1} \in \mathbb{C}^{d\times d}. \quad (10)$$

In the final stage, the spatial frequency $\mu_i, \forall i \in [1..d]$ can be obtained as $\mu_i = \arg\left(\boldsymbol{\Omega}(i,i)\right)$.

## IV. Derivation of analytical performance for 1-D Standard ESPRIT in DFT Beamspace

In this section, we present the derivation of the performance analysis of 1-D ESPRIT in DFT beamspace.

Note that the noiseless received signal in the DFT beamspace can be written as

$$\boldsymbol{Y}_{\mathrm{DFT}} = \boldsymbol{W}_B^{\mathrm{H}} \cdot \boldsymbol{A} \cdot \boldsymbol{S} = \boldsymbol{U}_{\mathrm{s}} \boldsymbol{\Sigma}_{\mathrm{s}} \boldsymbol{V}_{\mathrm{s}}^{\mathrm{H}}, \quad (11)$$

where $\boldsymbol{A} \in \mathbb{C}^{M\times d}$ is the steering matrix of the impinging signals, $\boldsymbol{S} \in \mathbb{C}^{d\times N}$ contains the impinging signals, and $\boldsymbol{Y}_{\mathrm{DFT}} \in \mathbb{C}^{B\times N}$ denotes the received signals after applying the DFT beamspace transformation.

Next, we consider a perturbed received signal $\tilde{\boldsymbol{Y}}$ and establish the relation between the matrix with noise samples $\boldsymbol{Z}$ (perturbation term) introduced in (1) and the spatial error for the $i$-th source $\Delta\mu_i$.

### A. Perturbation of signal subspace

Following the derivations in [3], the subspace perturbation can be represented as leakage from the orthogonal subspace

$$\Delta\boldsymbol{U}_{\mathrm{s}} \approx \boldsymbol{U}_{\mathrm{n}} \boldsymbol{K} \quad \text{and} \quad \Delta\boldsymbol{U}_{\mathrm{n}} \approx \boldsymbol{U}_{\mathrm{s}} \boldsymbol{L}, \quad (12)$$

where the matrices $\boldsymbol{K}$ and $\boldsymbol{L}$ define the leakages into the orthogonal subspaces. They can be found via properties of the subspaces of the perturbed matrix for the received signal after the beamspace transformation $\tilde{\boldsymbol{Y}}_{\mathrm{DFT}}$ [3].

The perturbation of the noise subspace can be found as

$$\Delta\boldsymbol{U}_{\mathrm{n}} = -\boldsymbol{U}_{\mathrm{s}} \boldsymbol{\Sigma}_{\mathrm{s}}^{-1} \boldsymbol{V}_{\mathrm{s}}^{\mathrm{H}} \Delta\boldsymbol{Y}_{\mathrm{DFT}}^{\mathrm{H}} \boldsymbol{U}_{\mathrm{n}}, \quad (13)$$

while the perturbation of the signal subspace is equal to

$$\Delta\boldsymbol{U}_{\mathrm{s}} = \boldsymbol{U}_{\mathrm{n}} \boldsymbol{U}_{\mathrm{n}}^{\mathrm{H}} \Delta\boldsymbol{Y}_{\mathrm{DFT}} \boldsymbol{V}_{\mathrm{s}} \boldsymbol{\Sigma}_{\mathrm{s}}^{-1}. \quad (14)$$

In the work, we use the perturbation of the signal subspace $\Delta\boldsymbol{U}_{\mathrm{s}}$ only since ESPRIT-type algorithms rely on the estimation of the signal subspace to find the target parameters.

### B. Perturbation of the shift-invariance equation

In the case of perturbed subspaces, the perturbation of the shift-invariance equation (8) can be written as

$$\begin{aligned} &\boldsymbol{G}_{1,B}\left(\boldsymbol{U}_{\mathrm{s}} + \Delta\boldsymbol{U}_{\mathrm{s}}\right)\left(\boldsymbol{\Upsilon} + \Delta\boldsymbol{\Upsilon}\right) = \boldsymbol{G}_{2,B}\left(\boldsymbol{U}_{\mathrm{s}} + \Delta\boldsymbol{U}_{\mathrm{s}}\right), \\ &\boldsymbol{G}_{1,B}\boldsymbol{U}_{\mathrm{s}}\Delta\boldsymbol{\Upsilon} + \boldsymbol{G}_{1,B}\Delta\boldsymbol{U}_{\mathrm{s}}\boldsymbol{\Upsilon} \approx \boldsymbol{G}_{2,B}\Delta\boldsymbol{U}_{\mathrm{s}}, \end{aligned} \quad (15)$$

where we have dropped the second-order terms. As a result, the perturbation of the matrix $\boldsymbol{\Upsilon}$ is equal to

$$\Delta\boldsymbol{\Upsilon} = \left(\boldsymbol{G}_{1,B}\boldsymbol{U}_{\mathrm{s}}\right)^{+}\left(\boldsymbol{G}_{2,B}\Delta\boldsymbol{U}_{\mathrm{s}} - \boldsymbol{G}_{1,B}\Delta\boldsymbol{U}_{\mathrm{s}}\boldsymbol{\Upsilon}\right). \quad (16)$$

### C. Perturbation of eigenvalues

At the next stage, we derive the expression for the perturbation of the eigenvalues of the matrix $\boldsymbol{\Upsilon}$.

$$\boldsymbol{\Upsilon} = \boldsymbol{Q}\boldsymbol{\Lambda}\boldsymbol{Q}^{-1} = \boldsymbol{T}\boldsymbol{\Omega}\boldsymbol{T}^{-1}. \quad (17)$$

Following [15], we can link the perturbation of the original matrix and the corresponding eigenvalues via

$$\boldsymbol{\Upsilon} + \Delta\boldsymbol{\Upsilon} = \boldsymbol{Q}\boldsymbol{\Lambda}\boldsymbol{Q}^{-1} + \boldsymbol{Q}\,\Delta\boldsymbol{\Lambda}\,\boldsymbol{Q}^{-1} + \mathcal{O}\left(\boldsymbol{\Delta}^2\right). \quad (18)$$

Taking into account that $\boldsymbol{\Upsilon} = \boldsymbol{Q}\boldsymbol{\Lambda}\boldsymbol{Q}^{-1}$ and keeping only the first-order terms of the expansion (18) we obtain

$$\Delta\boldsymbol{\Lambda} \approx \underbrace{\boldsymbol{Q}^{-1}}_{\boldsymbol{P}^{\mathrm{H}}} \Delta\boldsymbol{\Upsilon}\boldsymbol{Q}, \quad (19)$$

$$\boldsymbol{G}_{1,M} = \begin{bmatrix} 1 & \mathrm{e}^{-j\frac{\pi}{M}} & 0 & \cdots & 0 & 0 \\ 0 & \mathrm{e}^{-j\frac{\pi}{M}} & \mathrm{e}^{-j\frac{2\pi}{M}} & \cdots & 0 & 0 \\ 0 & 0 & \mathrm{e}^{-j\frac{2\pi}{M}} & \cdots & 0 & 0 \\ \vdots & \vdots & \vdots & \ddots & \vdots & \vdots \\ 0 & 0 & 0 & \cdots & \mathrm{e}^{-j(M-2)\frac{\pi}{M}} & \mathrm{e}^{-j(M-1)\frac{\pi}{M}} \\ (-1)^M & 0 & 0 & \cdots & 0 & \mathrm{e}^{-j(M-1)\frac{\pi}{M}} \end{bmatrix} \text{ and } \boldsymbol{G}_{2,M} = \begin{bmatrix} 1 & \mathrm{e}^{j\frac{\pi}{M}} & 0 & \cdots & 0 & 0 \\ 0 & \mathrm{e}^{j\frac{\pi}{M}} & \mathrm{e}^{j\frac{2\pi}{M}} & \cdots & 0 & 0 \\ 0 & 0 & \mathrm{e}^{j\frac{2\pi}{M}} & \cdots & 0 & 0 \\ \vdots & \vdots & \vdots & \ddots & \vdots & \vdots \\ 0 & 0 & 0 & \cdots & \mathrm{e}^{j(M-2)\frac{\pi}{M}} & \mathrm{e}^{j(M-1)\frac{\pi}{M}} \\ (-1)^M & 0 & 0 & \cdots & 0 & \mathrm{e}^{j(M-1)\frac{\pi}{M}} \end{bmatrix} \tag{7}$$

which brings us to the following expression for the $i$-th eigenvalue

$$\Delta\lambda_i \approx \boldsymbol{p}_i^{\mathrm{H}} \Delta\boldsymbol{\Upsilon} \boldsymbol{q}_i, \tag{20}$$

where we substitute the expression (16) and use the definition $\boldsymbol{\Upsilon}\boldsymbol{q}_i = \lambda_i \boldsymbol{q}_i$

$$\begin{aligned} \Delta\lambda_i &\approx \boldsymbol{p}_i^{\mathrm{H}} \left(\boldsymbol{G}_{1,B}\boldsymbol{U}_{\mathrm{s}}\right)^{+} \left(\boldsymbol{G}_{2,B}\Delta\boldsymbol{U}_{\mathrm{s}} - \boldsymbol{G}_{1,B}\Delta\boldsymbol{U}_{\mathrm{s}}\boldsymbol{\Upsilon}\right)\boldsymbol{q}_i, \\ &= \boldsymbol{p}_i^{\mathrm{H}} \left(\boldsymbol{G}_{1,B}\boldsymbol{U}_{\mathrm{s}}\right)^{+} \left(\boldsymbol{G}_{2,B}\Delta\boldsymbol{U}_{\mathrm{s}} - \lambda_i\boldsymbol{G}_{1,B}\Delta\boldsymbol{U}_{\mathrm{s}}\right)\boldsymbol{q}_i, \\ &= \boldsymbol{p}_i^{\mathrm{H}} \left(\boldsymbol{G}_{1,B}\boldsymbol{U}_{\mathrm{s}}\right)^{+} \left(\boldsymbol{G}_{2,B} - \lambda_i\boldsymbol{G}_{1,B}\right)\Delta\boldsymbol{U}_{\mathrm{s}}\boldsymbol{q}_i. \end{aligned} \tag{21}$$

### *D. Perturbation of spatial frequencies and angles*

The eigenvalues of the matrix $\boldsymbol{\Upsilon}$ are the complex-valued exponential functions in the form of $\mathrm{e}^{j\mu_i}$, where $\mu_i$ is the spatial frequency for the $i$-th source. The Taylor expansion for the $i$-th eigenvalue can be written as

$$\begin{aligned} \mathrm{e}^{j(\mu_i+\Delta\mu_i)} &= \mathrm{e}^{j\mu_i} + j\Delta\mu_i \cdot \mathrm{e}^{j\mu_i} + \mathcal{O}\left(\Delta^2\right) \\ &\approx \lambda_i + j\Delta\mu_i\lambda_i. \end{aligned} \tag{22}$$

Therefore, for small perturbations of the eigenvalues, we can write

$$\begin{aligned} &\lambda_i + \Delta\lambda_i = \lambda_i + j\Delta\mu_i\lambda_i, \\ &\Delta\lambda_i = j\Delta\mu_i\lambda_i \;\rightarrow\; \Delta\mu_i = \mathrm{Im}\left(\frac{\Delta\lambda_i}{\lambda_i}\right). \end{aligned} \tag{23}$$

As a result, we get a complete set of expressions to describe the performance of ESPRIT-type algorithms in DFT beamspace. The complete expression (24) is found by substituting the expression (14) in (21) and then in (23). It depends only on the instantaneous realization of the perturbation term $\Delta\boldsymbol{Y}_{\mathrm{DFT}}$, i.e., it does not rely on statistics.

A similar expression was derived in [3] for the element space version of the ESPRIT algorithm.

### *E. Perturbation of spatial frequencies in terms of physical parameters*

In this section, we further simplify the expression (24) following [16]. We can see from the expression (17) that the matrix $\boldsymbol{T}$ collects the right eigenvectors of the matrix $\boldsymbol{\Upsilon}$, while $\boldsymbol{T}^{-1}$ collects the left eigenvectors of the matrix. Using this observation, we can redefine the $i$-th pair of eigenvectors $\boldsymbol{p}_i$ and $\boldsymbol{q}_i$ as

$$\boldsymbol{p}_i^{\mathrm{H}} = \boldsymbol{e}_i^{\mathrm{T}}\boldsymbol{T}^{-1} \quad \text{and} \quad \boldsymbol{q}_i = \boldsymbol{T}\,\boldsymbol{e}_i, \tag{25}$$

where $\boldsymbol{e}_i \in \mathbb{R}^d$ is the unit vector which corresponds to the $i$-th column of the identity matrix $\boldsymbol{I}_d$. We also take into account that the matrix $\boldsymbol{T}$ converts the signal subspace into the beamspace steering matrix, i.e., $\boldsymbol{B} = \boldsymbol{U}_{\mathrm{s}}\boldsymbol{T}$. Then we can rewrite (21) as

$$\Delta\mu_i = \mathrm{Im}\left(\boldsymbol{e}_i^{\mathrm{T}}\boldsymbol{T}^{-1}\left(\boldsymbol{G}_{1,B}\boldsymbol{U}_{\mathrm{s}}\right)^{+}\left(\frac{1}{\lambda_i}\boldsymbol{G}_{2,B} - \boldsymbol{G}_{1,B}\right)\Delta\boldsymbol{U}_{\mathrm{s}}\boldsymbol{T}\boldsymbol{e}_i\right). \tag{26}$$

We can observe that on the one hand

$$\boldsymbol{T}^{-1}\left(\boldsymbol{G}_{1,B}\boldsymbol{U}_{\mathrm{s}}\right)^{+} = \left(\boldsymbol{G}_{1,B}\boldsymbol{U}_{\mathrm{s}}\boldsymbol{T}\right)^{+} = \left(\boldsymbol{G}_{1,B}\boldsymbol{B}\right)^{+} \tag{27}$$

and on the other hand

$$\begin{aligned} \boldsymbol{e}_i^{\mathrm{T}}\frac{1}{\lambda_i}\boldsymbol{T}^{-1}\left(\boldsymbol{G}_{1,B}\boldsymbol{U}_{\mathrm{s}}\right)^{+} &= \boldsymbol{e}_i^{\mathrm{T}}\boldsymbol{\Omega}^{-1}\left(\boldsymbol{G}_{1,B}\boldsymbol{U}_{\mathrm{s}}\boldsymbol{T}\right)^{+} \\ &= \boldsymbol{e}_i^{\mathrm{T}}\left(\boldsymbol{G}_{1,B}\boldsymbol{B}\boldsymbol{\Omega}\right)^{+} = \boldsymbol{e}_i^{\mathrm{T}}\left(\boldsymbol{G}_{2,B}\boldsymbol{B}\right)^{+}. \end{aligned} \tag{28}$$

As a result, we can write

$$\Delta\mu_i = \mathrm{Im}\left(\boldsymbol{e}_i^{\mathrm{T}}\left(\left(\boldsymbol{G}_{2,B}\boldsymbol{B}\right)^{+}\boldsymbol{G}_{2,B} - \left(\boldsymbol{G}_{1,B}\boldsymbol{B}\right)^{+}\boldsymbol{G}_{1,B}\right)\Delta\boldsymbol{U}_{\mathrm{s}}\boldsymbol{T}\boldsymbol{e}_i\right). \tag{29}$$

The expression (29) can be further simplified if we follow [16] and take into account that $\Delta\boldsymbol{U}_{\mathrm{s}} = \boldsymbol{U}_{\mathrm{n}}\boldsymbol{U}_{\mathrm{n}}^{\mathrm{H}}\Delta\boldsymbol{Y}_{\mathrm{DFT}}\boldsymbol{V}_{\mathrm{s}}\boldsymbol{\Sigma}_{\mathrm{s}}^{-1}$ and $\left(\left(\boldsymbol{G}_{2,B}\boldsymbol{B}\right)^{+}\boldsymbol{G}_{2,B} - \left(\boldsymbol{G}_{1,B}\boldsymbol{B}\right)^{+}\boldsymbol{G}_{1,B}\right)\boldsymbol{B} = \boldsymbol{0}$, i.e., the term belongs to the left-nullspace of $\boldsymbol{B}$. As a result we can drop the additional projection onto the noise subspace $\boldsymbol{U}_{\mathrm{n}}\boldsymbol{U}_{\mathrm{n}}^{\mathrm{H}}$. It leads to

$$\Delta\mu_i = \mathrm{Im}\left(\boldsymbol{e}_i^{\mathrm{T}}\left(\left(\boldsymbol{G}_{2,B}\boldsymbol{B}\right)^{+}\boldsymbol{G}_{2,B} - \left(\boldsymbol{G}_{1,B}\boldsymbol{B}\right)^{+}\boldsymbol{G}_{1,B}\right)\Delta\boldsymbol{Y}_{\mathrm{DFT}}\boldsymbol{V}_{\mathrm{s}}\boldsymbol{\Sigma}_{\mathrm{s}}^{-1}\boldsymbol{T}\boldsymbol{e}_i\right). \tag{30}$$

We can also rewrite the right part of the expression (30) as

$$\boldsymbol{V}_{\mathrm{s}}\boldsymbol{\Sigma}_{\mathrm{s}}^{-1}\boldsymbol{T}\boldsymbol{e}_i = \boldsymbol{V}_{\mathrm{s}}\boldsymbol{\Sigma}_{\mathrm{s}}^{-1}\boldsymbol{U}_{\mathrm{s}}^{\mathrm{H}}\boldsymbol{U}_{\mathrm{s}}\boldsymbol{T}\boldsymbol{e}_i = \boldsymbol{Y}_{\mathrm{DFT}}^{+}\boldsymbol{B}\boldsymbol{e}_i. \tag{31}$$

To simplify this expression, we introduce the auxiliary variables

$$\boldsymbol{\alpha}_i^{\mathrm{T}} = \sqrt{M}\boldsymbol{e}_i^{\mathrm{T}}\left(\left(\boldsymbol{G}_{2,B}\boldsymbol{B}\right)^{+}\boldsymbol{G}_{2,B} - \left(\boldsymbol{G}_{1,B}\boldsymbol{B}\right)^{+}\boldsymbol{G}_{1,B}\right) \in \mathbb{C}^{1\times B} \tag{32}$$

and

$$\boldsymbol{\beta}_i = \boldsymbol{Y}_{\mathrm{DFT}}^{+}\boldsymbol{B}\boldsymbol{e}_i \in \mathbb{C}^{N}. \tag{33}$$

In this way, the perturbation of the $i$-th spatial frequency turns into

$$\begin{aligned} \Delta\mu_i &= \mathrm{Im}\left(c\cdot\boldsymbol{\alpha}_i^{\mathrm{T}}\cdot\Delta\boldsymbol{Y}_{\mathrm{DFT}}\cdot\boldsymbol{\beta}_i\right) \\ &= \mathrm{Im}\left(c\cdot\left(\boldsymbol{\beta}_i\otimes\boldsymbol{\alpha}_i\right)^{\mathrm{T}}\cdot\mathrm{vec}\left\{\Delta\boldsymbol{Y}_{\mathrm{DFT}}\right\}\right) \\ &= \mathrm{Im}\left(c\cdot\left(\boldsymbol{\beta}_i\otimes\boldsymbol{\alpha}_i\right)^{\mathrm{T}}\cdot\Delta\boldsymbol{y}_{\mathrm{DFT}}\right), \end{aligned} \tag{34}$$

where $\Delta\boldsymbol{y}_{\mathrm{DFT}} = \mathrm{vec}\left\{\Delta\boldsymbol{Y}_{\mathrm{DFT}}\right\} \in \mathbb{C}^{BN}$ and $c = \frac{1}{\sqrt{M}}$.

In fact, the expression (34) uses the quantities $c$, $\boldsymbol{\alpha}_i$ and $\boldsymbol{\beta}_i$ that are written only in terms of physical parameters. It can already be

$$\Delta\mu_i = \mathrm{Im}\left(\boldsymbol{p}_i^{\mathrm{H}}\left(\boldsymbol{G}_{1,B}\boldsymbol{U}_{\mathrm{s}}\right)^{+}\left(\frac{1}{\lambda_i}\boldsymbol{G}_{2,B} - \boldsymbol{G}_{1,B}\right)\underbrace{\boldsymbol{U}_{\mathrm{n}}\boldsymbol{U}_{\mathrm{n}}^{\mathrm{H}}\Delta\boldsymbol{Y}_{\mathrm{DFT}}\boldsymbol{V}_{\mathrm{s}}\boldsymbol{\Sigma}_{\mathrm{s}}^{-1}}_{\Delta\boldsymbol{U}_{\mathrm{s}}}\boldsymbol{q}_i\right) \tag{24}$$

used to evaluate numerically the performance of 1-D ESPRIT in DFT beamspace.

In the next section, we analyze the statistical properties of this expression.

## V. Statistical analysis of the perturbation error

### A. Mean value

Assuming zero-mean perturbations $\mathbb{E}\{\Delta \boldsymbol{y}_{\mathrm{DFT}}\} = \mathbf{0}$, the mean value of the error $\Delta\mu_i$ can be written as

$$\begin{aligned}\mathbb{E}\{\Delta\mu_i\} &= \mathbb{E}\left\{\mathrm{Im}\left(c\cdot(\boldsymbol{\beta}_i\otimes\boldsymbol{\alpha}_i)^{\mathrm{T}}\cdot\Delta\boldsymbol{y}_{\mathrm{DFT}}\right)\right\}\\ &= \mathrm{Im}\left(c\cdot(\boldsymbol{\beta}_i\otimes\boldsymbol{\alpha}_i)^{\mathrm{T}}\cdot\mathbb{E}\{\Delta\boldsymbol{y}_{\mathrm{DFT}}\}\right)\\ &= \mathrm{Im}\left(c\cdot(\boldsymbol{\beta}_i\otimes\boldsymbol{\alpha}_i)^{\mathrm{T}}\cdot\mathbf{0}\right)=0. \end{aligned} \tag{35}$$

Analyzing the mean value of the first-order perturbation extension, we can conclude that 1-D ESPRIT in DFT beamspace is an unbiased estimator.

### B. Variance

The mean squared error (MSE) of the $i$-th source can be found as $\mathrm{MSE} = \mathbb{E}\left\{\Delta\mu_i^2\right\}$. We can write it explicitly in terms of the available parameters if we substitute in it the expression (34), i.e.,

$$\begin{aligned}\mathbb{E}\left\{\Delta\mu_i^2\right\} =& \mathbb{E}\Big\{\mathrm{Im}\left(c\cdot(\boldsymbol{\beta}_i\otimes\boldsymbol{\alpha}_i)^{\mathrm{T}}\cdot\Delta\boldsymbol{y}_{\mathrm{DFT}}\right)\\ &\times\mathrm{Im}\left(\Delta\boldsymbol{y}_{\mathrm{DFT}}^{\mathrm{T}}\cdot(\boldsymbol{\beta}_i\otimes\boldsymbol{\alpha}_i)\cdot c\right)\Big\}. \end{aligned} \tag{36}$$

Then we can show that for any complex number $z\in\mathbb{C}$ the following equality holds $\mathrm{Im}(z)\,\mathrm{Im}(z) = \frac{1}{2}\mathrm{Re}(zz^*) - \frac{1}{2}\mathrm{Re}(zz)$ and we can write

$$\begin{aligned}&\mathbb{E}\left\{\Delta\mu_i^2\right\} =\\ &= \frac{1}{2}c^2\,\mathrm{Re}\left((\boldsymbol{\beta}_i\otimes\boldsymbol{\alpha}_i)^{\mathrm{T}}\,\mathbb{E}\left\{\Delta\boldsymbol{y}_{\mathrm{DFT}}\Delta\boldsymbol{y}_{\mathrm{DFT}}^{\mathrm{H}}\right\}(\boldsymbol{\beta}_i\otimes\boldsymbol{\alpha}_i)^*\right)\\ &- \frac{1}{2}c^2\,\mathrm{Re}\left((\boldsymbol{\beta}_i\otimes\boldsymbol{\alpha}_i)^{\mathrm{T}}\,\mathbb{E}\left\{\Delta\boldsymbol{y}_{\mathrm{DFT}}\Delta\boldsymbol{y}_{\mathrm{DFT}}^{\mathrm{T}}\right\}(\boldsymbol{\beta}_i\otimes\boldsymbol{\alpha}_i)\right), \end{aligned} \tag{37}$$

which is the last stage that we can obtain without any assumptions about the statistics of the perturbation.

### C. Special case of ZMCSCG noise

Next, we assume that samples of noise are drawn from a zero mean circularly symmetric complex Gaussian (ZMCSCG) distribution with variance $\sigma_z^2$. We also take into account the structure of the perturbation vector, namely

$$\Delta\boldsymbol{y}_{\mathrm{DFT}} = \mathrm{vec}\{\Delta\boldsymbol{Y}_{\mathrm{DFT}}\} = \mathrm{vec}\left\{\boldsymbol{W}_B^{\mathrm{H}}\boldsymbol{Z}\right\} = \left(\boldsymbol{I}_N\otimes\boldsymbol{W}_B^{\mathrm{H}}\right)\cdot\boldsymbol{z}, \tag{38}$$

where $\boldsymbol{z} = \mathrm{vec}\{\boldsymbol{Z}\}\in\mathbb{C}^{MN}$ is the vectorization of the original perturbation matrix. Then the following expression holds

$$\begin{aligned}&\mathbb{E}\left\{\Delta\boldsymbol{y}_{\mathrm{DFT}}\Delta\boldsymbol{y}_{\mathrm{DFT}}^{\mathrm{H}}\right\}\\ &= \left(\boldsymbol{I}_N\otimes\boldsymbol{W}_B^{\mathrm{H}}\right)\cdot\underbrace{\mathbb{E}\left\{\boldsymbol{z}\boldsymbol{z}^{\mathrm{H}}\right\}}_{\sigma_z^2\boldsymbol{I}_{MN}}\cdot(\boldsymbol{I}_N\otimes\boldsymbol{W}_B) = M\sigma_z^2\boldsymbol{I}_{BN}, \end{aligned} \tag{39}$$

where we take into account that $\boldsymbol{W}_B^{\mathrm{H}}\boldsymbol{W}_B = M\boldsymbol{I}_B$ and $B$ is the number of beams. We can also show that the second term vanishes,

$$\begin{aligned}&\mathbb{E}\left\{\Delta\boldsymbol{y}_{\mathrm{DFT}}\Delta\boldsymbol{y}_{\mathrm{DFT}}^{\mathrm{T}}\right\}\\ &= \left(\boldsymbol{I}_N\otimes\boldsymbol{W}_B^{\mathrm{H}}\right)\cdot\underbrace{\mathbb{E}\left\{\boldsymbol{z}\boldsymbol{z}^{\mathrm{T}}\right\}}_{\mathbf{0}_{MN}}\cdot(\boldsymbol{I}_N\otimes\boldsymbol{W}_B^*) = \mathbf{0}. \end{aligned} \tag{40}$$

Therefore, the expression of the MSE of 1-D Standard ESPRIT in DFT beamspace (SBE) can be significantly simplified to

$$\mathrm{MSE}_{\mathrm{SBE}} = \mathbb{E}\left\{\Delta\mu_i^2\right\} = \frac{\sigma_z^2}{2}\left\|\boldsymbol{\alpha}_i\right\|_2^2\left\|\boldsymbol{\beta}_i\right\|_2^2, \tag{41}$$

where we also take into account that $c^2M = 1$.

Next, we show, how we can further simplify the expression (41) by rewriting $\left\|\boldsymbol{\beta}_i\right\|_2^2$ in terms of physical parameters as

$$\begin{aligned}\left\|\boldsymbol{\beta}_i\right\|_2^2 &= \boldsymbol{\beta}_i^{\mathrm{H}}\boldsymbol{\beta}_i = \boldsymbol{e}_i^{\mathrm{T}}\boldsymbol{B}^{\mathrm{H}}\left(\boldsymbol{Y}_{\mathrm{DFT}}^{+}\right)^{\mathrm{H}}\boldsymbol{Y}_{\mathrm{DFT}}^{+}\boldsymbol{B}\boldsymbol{e}_i\\ &= \boldsymbol{e}_i^{\mathrm{T}}\boldsymbol{B}^{\mathrm{H}}(\boldsymbol{B}^{\mathrm{H}})^{+}\left(\boldsymbol{S}\boldsymbol{S}^{\mathrm{H}}\right)^{+}\boldsymbol{B}^{+}\boldsymbol{B}\boldsymbol{e}_i = \frac{1}{N}\boldsymbol{e}_i^{\mathrm{T}}\hat{\boldsymbol{R}}_{\mathrm{s}}^{-1}\boldsymbol{e}_i, \end{aligned} \tag{42}$$

where $\hat{\boldsymbol{R}}_{\mathrm{s}} = \frac{1}{N}\boldsymbol{S}\boldsymbol{S}^{\mathrm{H}}$ is the estimate of the data covariance matrix.

In the current form (42), $\left\|\boldsymbol{\beta}_i\right\|_2^2$ is a random variable since it depends on the instantaneous realization of the random matrix $\boldsymbol{S}$. For the MSE we need to calculate the expectation over random realizations of signals in $\boldsymbol{S}$, i.e.,

$$\mathbb{E}\left\{\left\|\boldsymbol{\beta}_i\right\|_2^2\right\} = \frac{1}{N}\boldsymbol{e}_i^{\mathrm{T}}\,\mathbb{E}\left\{\hat{\boldsymbol{R}}_{\mathrm{s}}^{-1}\right\}\,\boldsymbol{e}_i, \tag{43}$$

which we can rewrite using the Neumann series and assuming that the perturbation $\Delta\boldsymbol{R} = \hat{\boldsymbol{R}} - \boldsymbol{R}$ of the covariance matrix $\boldsymbol{R}$ is zero-mean and small enough so that we can only consider the first-order term to approximate the inverse

$$\begin{aligned}\mathbb{E}\left\{\hat{\boldsymbol{R}}_{\mathrm{s}}^{-1}\right\} &= \mathbb{E}\left\{(\boldsymbol{R}_{\mathrm{s}}+\Delta\boldsymbol{R}_{\mathrm{s}})^{-1}\right\}\\ &\approx \mathbb{E}\left\{\boldsymbol{R}_{\mathrm{s}}^{-1} - \boldsymbol{R}_{\mathrm{s}}^{-1}\Delta\boldsymbol{R}_{\mathrm{s}}\boldsymbol{R}_{\mathrm{s}}^{-1}\right\} = \boldsymbol{R}_{\mathrm{s}}^{-1}, \end{aligned} \tag{44}$$

since $\mathbb{E}\{\Delta\boldsymbol{R}_{\mathrm{s}}\} = \mathbf{0}$.

As a result, the expression for the MSE in terms of physical parameters can be written as

$$\mathrm{MSE}_{\mathrm{SBE}} = \frac{\sigma_z^2}{2N}\cdot\left\|\boldsymbol{\alpha}_i\right\|_2^2\cdot\left(\boldsymbol{R}_{\mathrm{s}}^{-1}\right)_{\kappa,\kappa}. \tag{45}$$

### D. Special case of a single source

In the case of a single source ($d=1$) we can derive the expression for $\left\|\boldsymbol{\alpha}_1\right\|_2^2$ in a closed form.

We consider case of two consecutive beams $b_\kappa$ and $b_{\kappa+1}$, i.e., $\boldsymbol{B} = [\ b_\kappa,\ \ b_{\kappa+1}\ ]^{\mathrm{T}}$. In this way, the selection matrices $\boldsymbol{G}_{1,2}$ and $\boldsymbol{G}_{2,2}$ can be written as

$$\boldsymbol{G}_{1,2} = \left[\ \mathrm{e}^{-j\frac{\gamma_\kappa}{2}},\ \mathrm{e}^{-j\frac{\gamma_{\kappa+1}}{2}}\ \right]\ \text{and}\ \boldsymbol{G}_{2,2} = \left[\ \mathrm{e}^{j\frac{\gamma_\kappa}{2}},\ \mathrm{e}^{j\frac{\gamma_{\kappa+1}}{2}}\ \right]. \tag{46}$$

Inserting $\boldsymbol{B}$, $\boldsymbol{G}_{1,2}$, and $\boldsymbol{G}_{2,2}$ in (32), the vector $\boldsymbol{\alpha}_1$ can be written as in (47). It leads us to the following expression of $\left\|\boldsymbol{\alpha}_1\right\|_2^2$

$$\left\|\boldsymbol{\alpha}_1\right\|_2^2 = \frac{4M\sin^2\left(\frac{\pi}{M}\right)\left(b_\kappa^2+b_{\kappa+1}^2\right)}{\left(b_\kappa^2+b_{\kappa+1}^2+2\cos\left(\frac{\pi}{M}\right)b_\kappa b_{\kappa+1}\right)^2}. \tag{48}$$

For the particular case, when the spatial frequency $\mu$ is chosen such that $b_\kappa(\mu) = b_{\kappa+1}(\mu)$ and $(\mu-\gamma_\kappa) = \frac{\pi}{M}$, i.e., the spatial frequency is in the middle between two beams, the expression can be further simplified to

$$\left\|\boldsymbol{\alpha}_1\right\|_2^2 = 2M\frac{\sin^4\left(\frac{1}{2}\frac{\pi}{M}\right)}{\cos^2\left(\frac{1}{2}\frac{\pi}{M}\right)}, \tag{49}$$

which in case of $M\gg 1$ can be approximated by the first order terms of the Taylor expansion for the numerator and the denominator as

$$\left\|\boldsymbol{\alpha}_1\right\|_2^2 \approx 2M\left(\frac{1}{2}\frac{\pi}{M}\right)^4 = \frac{\pi^4}{8M^3}, \tag{50}$$

this is the desired result which concludes the derivation.

The final expression for the MSE of 1-D Standard ESPRIT in DFT beamspace (SBE) in case of a single source can be written as

$$\mathrm{MSE}_{\mathrm{SBE}} = \frac{\sigma_z^2}{2}\cdot\frac{\pi^4}{8M^3N}\cdot\left(\boldsymbol{R}_{\mathrm{s}}^{-1}\right)_{(k,k)}. \tag{51}$$

$$\begin{aligned}\boldsymbol{\alpha}_1^{\mathrm{T}} &= \sqrt{M}\left[\frac{\mathrm{e}^{j\frac{\gamma_\kappa}{2}}}{\mathrm{e}^{j\frac{\gamma_\kappa}{2}}b_\kappa+\mathrm{e}^{j\frac{\gamma_{\kappa+1}}{2}}b_{\kappa+1}}-\frac{\mathrm{e}^{-j\frac{\gamma_\kappa}{2}}}{\mathrm{e}^{-j\frac{\gamma_\kappa}{2}}b_\kappa+\mathrm{e}^{-j\frac{\gamma_{\kappa+1}}{2}}b_{\kappa+1}}\;,\;\frac{\mathrm{e}^{j\frac{\gamma_{\kappa+1}}{2}}}{\mathrm{e}^{j\frac{\gamma_\kappa}{2}}b_\kappa+\mathrm{e}^{j\frac{\gamma_{\kappa+1}}{2}}b_{\kappa+1}}-\frac{\mathrm{e}^{-j\frac{\gamma_{\kappa+1}}{2}}}{\mathrm{e}^{-j\frac{\gamma_\kappa}{2}}b_\kappa+\mathrm{e}^{-j\frac{\gamma_{\kappa+1}}{2}}b_{\kappa+1}}\right]\\ &= \sqrt{M}\left[\frac{-2j\sin\left(\frac{\pi}{M}\right)b_{\kappa+1}}{b_\kappa^2+b_{\kappa+1}^2+2\cos\left(\frac{\pi}{M}\right)b_\kappa b_{\kappa+1}}\;,\;\frac{2j\sin\left(\frac{\pi}{M}\right)b_\kappa}{b_\kappa^2+b_{\kappa+1}^2+2\cos\left(\frac{\pi}{M}\right)b_\kappa b_{\kappa+1}}\right]\end{aligned} \tag{47}$$

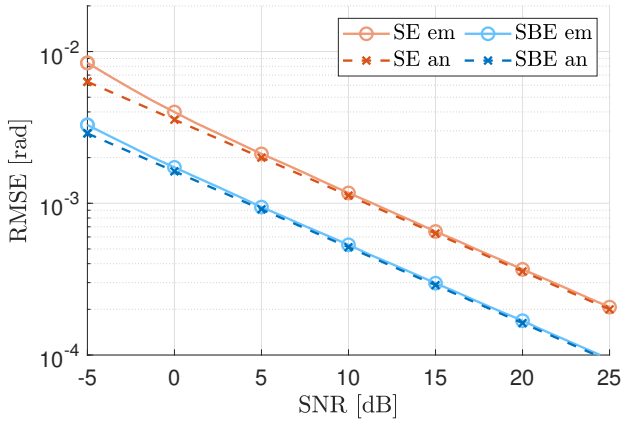


(a) RMSE versus SNR.

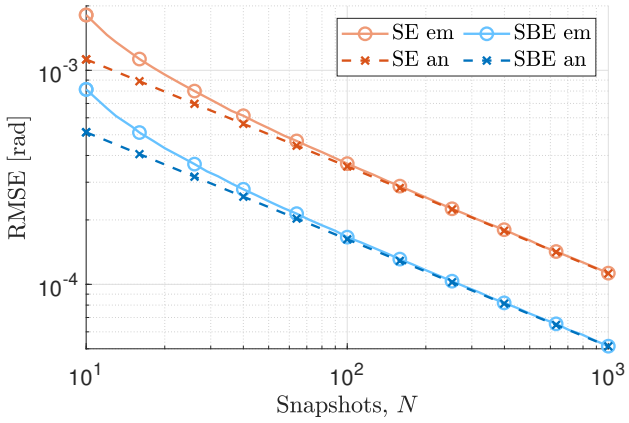


(b) RMSE versus number of snapshots.

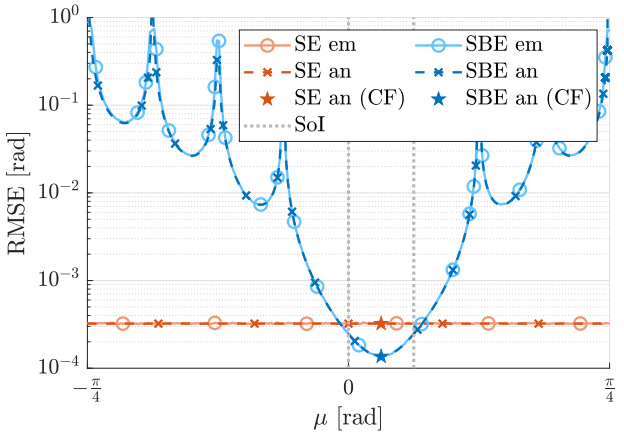


(c) RMSE versus spatial frequency.

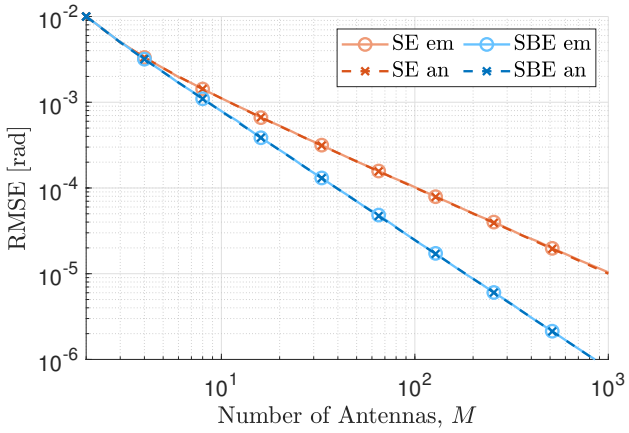


(d) RMSE versus number of antennas.

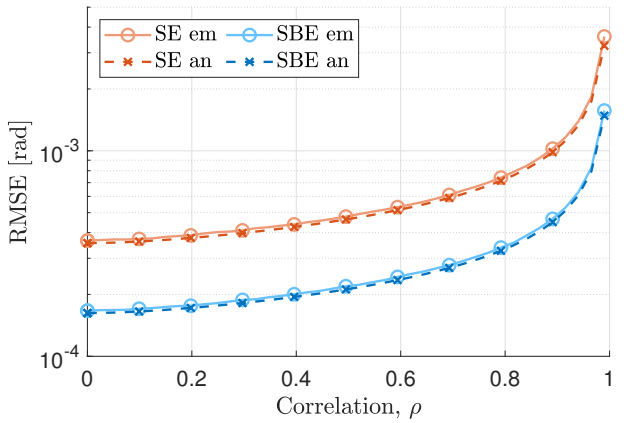


(e) RMSE versus correlation.

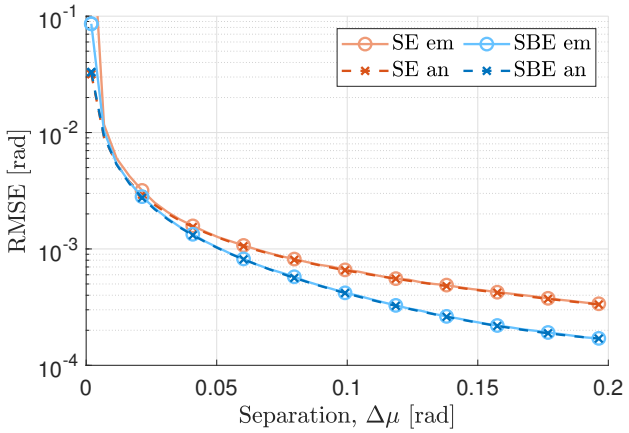


(f) RMSE versus spatial separation.

Fig. 2: Performance analysis for 1-D ESPRIT in DFT Beamspace in terms of physical parameters.

Note that in the case of the element space, the asymptotic performance of ESPRIT for a single source that is based on the first-order perturbation expansion [3] is given by the expression

$$\mathrm{MSE}_{\mathrm{SE}} = \frac{\sigma_z^2}{2} \cdot \frac{2}{(M-1)^2 N} \cdot \left(\boldsymbol{R}_{\mathrm{s}}^{-1}\right)_{(k,k)}. \tag{52}$$

Comparing (51) and (52) we can observe that the MSE for ESPRIT in DFT beamspace decreases by one order of magnitute faster than for element space ESPRIT as a function of $M$. In the next section, we confirm this observation via simulations.

## VI. Simulation results

In this section, we present the selected simulation results to demonstrate the validity of the derived expressions for the performance analysis of 1-D ESPRIT in DFT Beamspace. For the simulations, we consider a uniform linear array with $M = 32$ antennas with equidistant spacing $\frac{\lambda}{2}$. The number of snapshots is $N = 100$ samples unless otherwise stated. We use samples drawn from the zero-mean circularly symmetric complex Gaussian distribution for the perturbation matrix. We calculate the variance per element of the distribution as a function of the SNR, i.e., $\sigma_z^2 = 10^{-\frac{\mathrm{SNR}}{10}}$.

The estimation accuracy is measured in terms of the Root Mean Squared Error (RMSE) that is calculated using the expression

$$\mathrm{RMSE} = \sqrt{\mathbb{E}\left\{\frac{1}{d}\sum_{i=1}^{d}(\mu_i - \hat{\mu}_i)^2\right\}}. \tag{53}$$

We illustrate the empirical (`em`) RMSE in solid lines and the analytical (`an`) RMSE in dashed lines, which were obtained by averaging over different realizations of the perturbation. Also, we show all results for 1-D Standard ESPRIT (`SE`) in red and 1-D Beamspace ESPRIT (`SBE`) in blue. For Standard ESPRIT in element space [17], the performance analysis is taken from [3]. For the analytical performance of Beamspace ESPRIT (`SBE`), we use the expression (45). In all simulations, we build the beamforming matrix for the beamspace algorithm by selecting the 2 closest beams to each spatial frequency. We control the correlation between the sources via the parameter $\rho$ by defining the data correlation matrix as

$$\boldsymbol{R}_{\mathrm{s}} = \rho\mathbf{1} + (1-\rho)\boldsymbol{I}_d, \tag{54}$$

where $\mathbf{1}$ is a matrix of ones. We assume $\rho = 0$ unless otherwise stated. All simulations presented in this paper were averaged over 10000 realizations of random perturbations and data. For the presented simulations, we used the following realization of the spatial frequencies

$$\boldsymbol{\mu} = [\ -2.5,\ -2.3,\ 0.5,\ 2.1,\ 2.5,\ 3.1\ ]^{\mathrm{T}}, \tag{55}$$

unless otherwise stated. The key simulation parameters for each figure can be found in Table I.

In Figure 2(a), we show the behavior for different values of SNRs. We can observe that the simulation results follow the analytical prediction of beamspace ESPRIT. We can also notice a linear decrease on a logarithmic scale of the RMSE versus the SNR, as predicted by the expression (45).

TABLE I: Simulation parameters

| Figure | Parameters | | | | |
|---|---|---|---|---|---|
| 2(a) | $M = 32$ | $N = 100$ | - | $d = 6$ | $\rho = 0$ |
| 2(b) | $M = 32$ | - | $\mathrm{SNR} = 20\,\mathrm{dB}$ | $d = 6$ | $\rho = 0$ |
| 2(c) | $M = 32$ | $N = 100$ | $\mathrm{SNR} = 20\,\mathrm{dB}$ | $d = 1$ | $\rho = 0$ |
| 2(d) | - | $N = 100$ | $\mathrm{SNR} = 20\,\mathrm{dB}$ | $d = 1$ | $\rho = 0$ |
| 2(e) | $M = 32$ | $N = 100$ | $\mathrm{SNR} = 20\,\mathrm{dB}$ | $d = 6$ | - |
| 2(f) | $M = 32$ | $N = 100$ | $\mathrm{SNR} = 20\,\mathrm{dB}$ | $d = 2$ | $\rho = 0$ |

In Figure 2(b), we analyze the impact of the number of snapshots on the performance. We vary $N$ in the range of $[10...1000]$ snapshots. We can also observe a linear decrease on a logarithmic scale of the RMSE with an increase in the number of snapshots.

In Figure 2(c), the RMSE over a range of spatial frequencies is presented. Only two beams $b_0$ and $b_1$ are selected for the algorithm. The centers of the beams are shown with the gray dashed vertical lines. The space between the two centers forms the SoI. We observe a better performance in the SoI range and a rapid degradation outside of it. We notice that the expression (45) for the analytical performance is able to represent the behavior of the empirical results accurately enough. Additionally, we depict two special points that correspond to closed-form expressions in the case of a single source - the blue star point "`SBE an (CF)`" that corresponds to the RMSE of ESPRIT in DFT Beamspace (51) and the red star point "`SE an (CF)`" corresponds to the RMSE of ESPRIT in element space (52).

In Figure 2(d), we show the impact of the number of antennas on the performance. We choose $d = 1$ with the spatial frequency $\mu = \frac{\pi}{M}$, where $M$ is in the range $[2...2000]$. We can observe that the slope of the RMSE for the beamspace version of the algorithm is steeper, which is $\approx \mathcal{O}\left(M^{-1.5}\right)$ for beamspace ESPRIT versus $\approx \mathcal{O}\left(M^{-1}\right)$ for the element space counterpart. This result corresponds to the impact of $M$ in the analytical expressions (51) and (52).

In Figure 2(e), we present the dependence of the RMSE on the correlation between two sources. As expected, the correlation has an identical impact on ESPRIT in DFT beamspace and in element space. A better performance within the SoI range of ESPRIT in DFT beamspace can explain the shift between the lines.

In Figure 2(f), we depict the impact of the source separation on the performance. We consider two sources $\mu_1 = 0$ and $\mu_2 = \Delta\mu$. The total range is equal to $\Delta\mu \in \left[0, \frac{2\pi}{M}\right]$. We can observe a slightly better ability of ESPRIT in DFT beamspace to handle closely spaced sources than in element space. We use $B = 3$ closest beams to each spatial frequency during the sectorization procedure to determine the beamforming matrix.

Observing the simulations, we can confirm that the results based on Monte Carlo trials match the analytical expressions derived in the paper.

## VII. Conclusions and Future Directions

In this paper, we present an analytical performance assessment of 1-D ESPRIT in DFT Beamspace. A simplified expression for the mean squared error is derived in terms of the physical parameters. We show the impact of the beamspace transformation on the performance of the algorithm. The presented analytical expression allows us to predict with high accuracy the performance of 1-D ESPRIT in DFT Beamspace, especially for the range of high SNRs. Additionally, we present a simplified expression for the cases of perturbations caused by white noise and a single source.

The results presented in this paper can be extended to multiple dimensions to analyze the performance of multidimensional parameter estimation algorithms in DFT beamspace, such as Unitary Tensor-ESPRIT-type algorithms in DFT beamspace. An additional analysis of the impact of forward-backward-averaging (FBA) and spatial smoothing can be performed.

## REFERENCES


[1] F. Li and R. Vaccaro, "Analysis of Min-Norm and MUSIC with arbitrary array geometry," *IEEE Transactions on Aerospace and Electronic Systems*, vol. 26, no. 6, pp. 976–985, Nov. 1990.

[2] F. Li and R. J. Vaccaro, "Unified analysis for DOA estimation algorithms in array signal processing," *Signal Processing*, vol. 25, no. 2, pp. 147–169, Nov. 1991.

[3] F. Li, H. Liu, and R. J. Vaccaro, "Performance analysis for DOA estimation algorithms: Unification, simplification, and observations," *IEEE Transactions on Aerospace and Electronic Systems*, vol. 29, no. 4, pp. 1170–1184, 1993.

[4] F. Roemer, H. Becker, M. Haardt, and M. Weis, "Analytical performance evaluation for HOSVD-based parameter estimation schemes," in *Proc. 3rd IEEE International Workshop on Computational Advances in Multi-Sensor Adaptive Processing (CAMSAP-09)*, Dec. 2009, pp. 77–80.

[5] F. Roemer, H. Becker, and M. Haardt, "Analytical performance assessment for multi-dimensional Tensor-ESPRIT-type parameter estimation algorithms," in *Proc. International Conference on Acoustics, Speech and Signal Processing (ICASSP-10)*, Dallas, TX, USA, 2010, pp. 2598–2601.

[6] F. Roemer, M. Haardt, and G. Del Galdo, "Analytical Performance Assessment of Multi-Dimensional Matrix- and Tensor-Based ESPRIT-Type Algorithms," *IEEE Transactions on Signal Processing*, vol. 62, no. 10, pp. 2611–2625, May 2014.

[7] E. R. Balda, S. A. Cheema, J. Steinwandt, M. Haardt, A. Weiss, and A. Yeredor, "First-order perturbation analysis of low-rank tensor approximations based on the truncated HOSVD," in *Proc. 50th Asilomar Conference on Signals, Systems and Computers (Asilomar-16)*, Nov. 2016, pp. 1723–1727.

[8] M. D. Zoltowski, M. Haardt, and C. P. Mathews, "Closed-form 2-D angle estimation with rectangular arrays in element space or beamspace via unitary ESPRIT," *IEEE Transactions on Signal Processing*, vol. 44, no. 2, pp. 316–328, 1996.

[9] C. Mathews, M. Haardt, and M. Zoltowski, "Performance analysis of closed-form, ESPRIT based 2-D angle estimator for rectangular arrays," *IEEE Signal Processing Letters*, vol. 3, no. 4, pp. 124–126, Apr. 1996.

[10] H. Liu and F. Li, "Statistical evaluation of beam-space direction-of-arrival estimators," in *Proc. International Conference on Acoustics, Speech, and Signal Processing (ICASSP-92)*, vol. 5, San Francisco, CA, USA, 1992, pp. 389–392.

[11] J. Zhang, D. Rakhimov, and M. Haardt, "Gridless Channel Estimation for Hybrid mmWave MIMO Systems via Tensor-ESPRIT Algorithms in DFT Beamspace," *IEEE Journal of Selected Topics in Signal Processing*, vol. 15, no. 3, pp. 816–831, 2021.

[12] D. J. Jeffries and D. R. Farrier, "Asymptotic results for eigenvector methods," *IEE Proceedings-F (Communications, Radar and Signal Processing)*, vol. 132, no. 7, pp. 589–594, Dec. 1985.

[13] D. Rakhimov, J. Zhang, A. L. F. Almeida, A. Nadeev, and M. Haardt, "Channel Estimation for Hybrid Multi-Carrier mmWave MIMO Systems Using 3-D Unitary Tensor-ESPRIT in DFT beamspace," in *Proc. 53rd Asilomar Conference on Signals, Systems, and Computers (Asilomar-19)*, Pacific Grove, CA, USA, 2019, pp. 447–451.

[14] D. Rakhimov, S. P. Deram, B. Sokal, K. Naskovska, A. de Almeida, and M. Haardt, "Iterative Tensor Receiver for MIMO-GFDM systems," in *Proc. 11th Sensor Array and Multichannel Signal Processing Workshop (SAM-20)*, Jun. 2020, pp. 1–5.

[15] G. W. Stewart and J.-G. Sun, *Matrix Perturbation Theory*. Elsevier Science, Jun. 1990.

[16] F. Li, H. Liu, and R. Vaccaro, "Performance analysis for DOA estimation algorithms using physical parameters," in *Proc. International Conference on Acoustics, Speech, and Signal Processing (ICASSP-92)*, vol. 2, Mar. 1992, pp. 537–540.

[17] A. Paulraj, R. Roy, and T. Kailath, "Estimation Of Signal Parameters Via Rotational Invariance Techniques - ESPRIT," in *Proc. 9th Asilomar Conference on Circuits, Systems and Computers (Asilomar-85)*, Nov. 1985, pp. 83–89.